

Structural and dynamical features of multiple metastable glassy states in a colloidal system with competing interactions

Christian L. Klix^{1,2}, C. Patrick Royall^{1,3} and Hajime Tanaka¹

¹Institute of Industrial Science, University of Tokyo,
Meguro-ku, Tokyo 153-8505, Japan.

²University of Konstanz, 78457 Konstanz, Germany.

³School of Chemistry, University of Bristol, Bristol BS8 1TS, UK.

Abstract

Systems in which a short-ranged attraction and long-ranged repulsion compete are intrinsically frustrated, leading their structure and dynamics to be dominated either by mesoscopic order or by metastable disorder. Here we report the latter case in a colloidal system with long-ranged electrostatic repulsions and short-ranged depletion attractions. We find a variety of states exhibiting slow non-diffusive dynamics: a gel, a glassy state of clusters, and a state reminiscent of a Wigner glass. Varying the interactions, we find a continuous crossover between the Wigner and cluster glassy states, and a sharp discontinuous transition between the Wigner glassy state and gel. This difference reflects the fact that dynamic arrest is driven by repulsion for the two glassy states and attraction in the case of the gel.

I. INTRODUCTION

In general, attractive interactions promote ordered phases or condensates, whereas long ranged repulsions inhibit this tendency, fundamentally redefining the system's free energy leading to complex phases that break translational and/or rotational symmetry. Such mesoscopic ordering occurs in a very diverse range of materials [1, 2], from the pasta phase in neutron stars [3], highly correlated quantum Hall and strongly correlated electron systems such as high T_c superconductors [2, 4] to classical systems [1] such as ferromagnetic films, diblock copolymers, colloids [5, 6], and biological systems. It has also been suggested [5–8] that competing interactions can also cause frustration, leading to exotic nonergodic disordered states. In the above examples, the system is able to relax on mesoscopic lengthscales; it is rather rare to see metastable disorder at the local level. Such disordered states were however reported for Laponite suspensions, where electrostatic repulsions compete with van der Waals attractions, but the anisotropic particles and interactions make the situation rather complex [9].

Spheres with a hard core repulsion and an attraction have long provided a model which captures the essence of atoms and small molecules. Short-ranged attractions lead to gelation due to arrested phase separation [10]. At higher densities both hard-sphere and attractive glasses are found [Fig. 1(g)] [11], along with gels [12]. Long-range repulsions can lead to glasses at low densities [13, 14], and combined with short-ranged attractions, the behavior is very rich and complex. Indeed, many properties of biological materials may be connected, fundamentally, to a short-range attraction and longer-ranged repulsion due to electrostatic charging from immersion in an aqueous medium [15]. For example globular proteins are rather well described as spheres with short-ranged attractions and long-ranged repulsions [16]. While most biological systems are much more complex than spheres with competing interactions, it is clearly important to understand this seemingly simple addition to well-studied models of atoms, not least as it offers insight into transitions between metastable states.

Since competing interactions lead to frustration between phase separation and homogeneity, a characteristic lengthscale is often predicted from computer simulation, for example, periodic lamellae [6] or low-dimensional clusters of a specific size [17]. These may then undergo hierarchical self-organization; in particular, clusters may themselves be implicated in

gelation [18] and undergo dynamical arrest to form a ‘cluster glass’ [19]. Despite recent developments [16, 20, 21], experimental work in colloidal systems with competing interactions has so far found little evidence of periodic structures, although gels with novel structures [20, 21] and low-dimensional clusters [20, 22] have been seen.

II. EXPERIMENTAL

We consider spherical colloids (diameter σ) immersed in a solvent, with a relatively strong, long-range electrostatic repulsion, and a short-range, tuneable attraction mediated by non-adsorbing polymer in which the strength of the attraction is set by the polymer concentration c_p , and the range by the polymer size, in this case the polymer-colloid size ratio $q \sim 0.19$ (see appendix). We determined the attractions in a very similar system [23], and the magnitude of the electrostatic repulsions from fitting the structure of equilibrium fluids [24] which gave a colloid charge number of $Z \sim 600 \pm 200$ (see appendix). According to mode-coupling theory for Yukawa systems [25], for our parameters we expect a transition to a Wigner glass at comparable colloid volume fractions to those observed experimentally. Mixing the samples prior to imaging leads to a randomized initial state, after which the tuned interactions and colloid volume fraction ϕ lead the system to a (metastable) point on the state diagram (Fig. 1). We sometimes see the formation of a Wigner crystal state at high $\phi > 0.2$ and low c_p ; however, this is a rare event [see Fig. 1(f)] and usually the system forms a metastable glassy state before crystallization can occur (see appendix). Using real space structural and dynamical analysis, we find a state diagram dominated by three types of glassy states with different disordered structures: Wigner glassy state, cluster glassy state, and gel. We study the transitions between these states, and reveal the nature of these transitions and its link to the interactions leading to slow dynamics.

III. RESULTS AND DISCUSSION

We begin by presenting the state diagram in Fig. 1, which underlines the extent to which the system is dominated by dynamically arrested states. A low-density colloidal fluid ($\phi = 0.002$) where the system is ergodic is shown in Fig. 1(c). Increasing the volume fraction to $\phi = 0.016$ results in a glassy state where the slow dynamics is driven by the

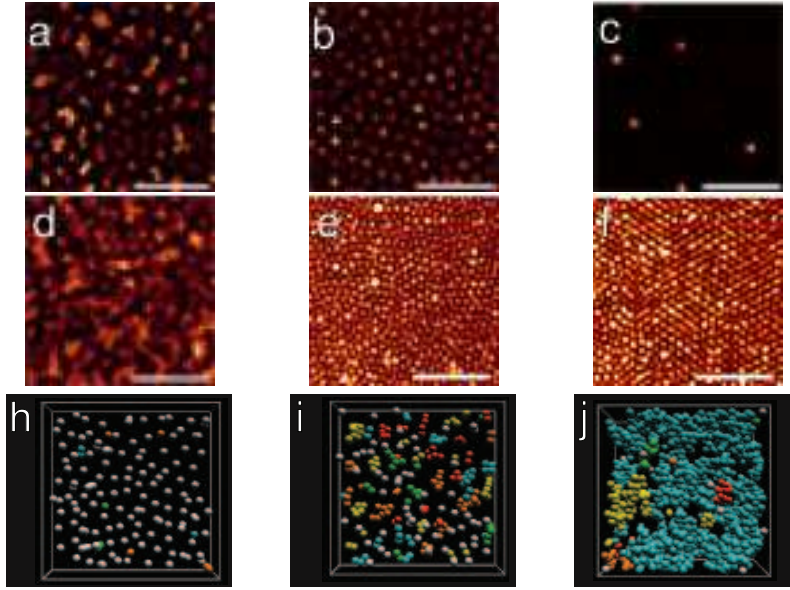
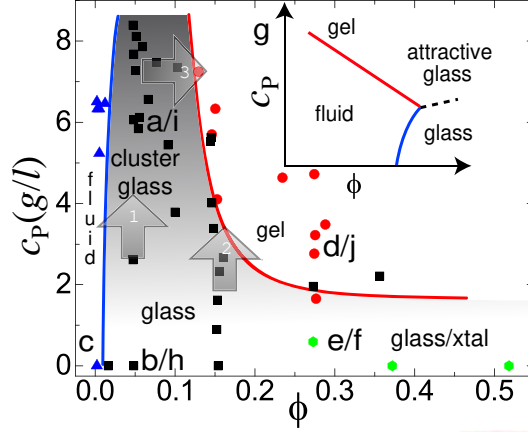


Figure 1: State diagram of the investigated system and 2D and 3D structures. (a) cluster glassy state, $\phi = 0.04$, $c_p = 8.39$ g/l. (b) Wigner glassy state, $\phi = 0.047$, $c_p = 0$. (c) fluid, $\phi = 0.002$, $c_p = 0$. (d) gel, $\phi = 0.152$, $c_p = 4.10$ g/l. (e) Wigner glass, $\phi = 0.372$, $c_p = 0$. (f) crystal, $\phi = 0.372$, $c_p = 0$. Bars are $20 \mu\text{m}$. Boundaries are guides to the eyes. Increasing grey shading represents increasing amount of clusters. Thick arrows denote paths 1-3 described in the text. Cluster glassy state is denoted by squares, gel by circles, crystal/glassy state by hexagons and fluid by triangles. Grey arrows indicate states for the images (a)-(f). (g) State diagram of a system without long-ranged repulsive interactions [11], showing two glassy states at high colloid concentration. (h)-(j): 3D structures of (h) Wigner glassy state, (i) cluster glassy state, and (j) gel. White particles have no neighbors, otherwise colors denote connected regions.

long-ranged electrostatic repulsions [Figs. 1(b), (e), and (h)]. We thus term this state a ‘Wigner glassy state’. At low ϕ and higher c_p , we see the formation of clusters and term this state a ‘cluster glassy state’ [Figs. 1(a) and (i)]. Meanwhile, increasing both c_p and ϕ results in a gel which we define through percolation [Figs. 1(d) and (j)], and appears dynamically arrested [Fig. 2(a)]. A typical state diagram for a colloidal system without electrostatic repulsions is schematically shown in Fig. 1(g). We see striking differences in the structure of the state diagram between systems with and without electrostatic repulsions (see also appendix). With electrostatics the ergodic region is very narrow, around $\phi \sim 0$, and the glassy states dominate the state diagram. There are three glassy states with very different structures: Wigner and cluster glassy states and a gel state. We also found three types of transitions between these states accompanied by local structural changes.

Before discussing the structure of these three states in more detail, let us consider the dynamics. Mean squared displacement (MSD) measurements, in which the colloids are tracked in two dimensions (2D), are shown in Fig. 2. What is clear is that the (ergodic) fluid we see at low ϕ appears to exhibit diffusive behavior, and the gel appears dynamically arrested, within the accuracy to which we can track the particles (100 nm or $\sigma/20$). The other states show extensive non-diffusive behavior, yet they do not reach a clear plateau on the experimental timescale although we track the particles for up to 20 hours for the cluster glassy state and up to 2 hours for the Wigner glassy state. We are limited in particle tracking at long times due to particle loss (particles diffusing out of our volume), bleaching and drift, along with residual sedimentation. We estimate the cage size as the width of the first and second peaks in $g(r)$ for the Wigner and cluster glassy states respectively [see Fig. 3(a)]. In the case of the gel the cage size is taken as the bond length, 0.19σ . Concerning the cluster glassy state, similar sub-diffusive behavior has recently been seen in computer simulation [19]. We note that such behavior is expected from the fact that clusters can rotate as rigid bodies [see Fig. 2(b)]. This strong decoupling between translational and rotational motion may be unique to a cluster glassy state. In the case of the Wigner glassy state, based upon simulation work in a similar system [26], we believe that our experimental timescales limit full access to relaxation phenomena. In any case, the cage size is not reached [see Fig. 2(a)]. The soft nature of the interactions is another factor which prolongs the sub-diffusive regime and thus makes a rigorous confirmation of nonergodicity very challenging. The non-diffusive behavior is suggestive of the glassiness of these states. Since we do not find a clear plateau

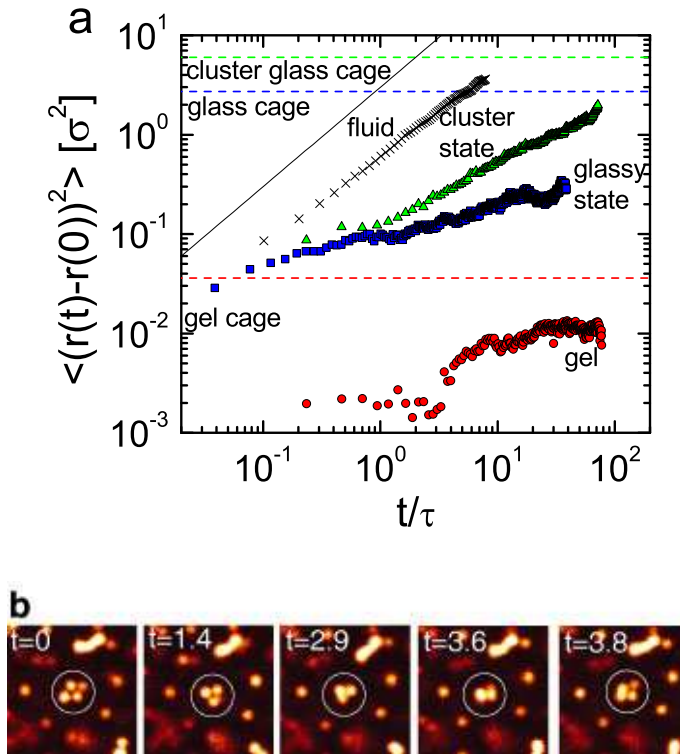


Figure 2: (a) Mean square displacements. Crosses=fluid ($\phi = 0.002$, $c_p = 0$), green triangles=cluster glassy state ($\phi = 0.051$, $c_p = 5.16$ g/l), red circles=gel ($\phi = 0.275$, $c_p = 4.88$ g/l) and blue squares=glassy state ($\phi = 0.069$, $c_p = 0$). τ =characteristic diffusion time (see appendix). Dashed lines corresponding to the cage size are plotted for gel (0.19σ), Wigner state (1.9σ) and cluster state (2.1σ), respectively. (b) Confocal microscope images of a cluster spinning in its ‘cage’. Time unit= τ , image width= $19.5 \mu\text{m}$.

experimentally, we term these ‘cluster glassy state’ and ‘Wigner glassy state’, respectively, although the states may be regarded as nonergodic at least practically.

The state diagram dominated by these three glassy states illustrated in Fig. 1 yields three transitions. It is a commonly held view that dynamical arrest is accompanied by little structural change. While literature on transitions between glassy states is scarce, the structural change in the attractive-repulsive glass transition at high packing fraction is rather subtle [27]. Conversely, all states identified here are characterized by their structures [see Figs. 1(h), (i), and (j)]. Our analysis shows a considerable variety of metastable structures in the response to small changes in parameters.

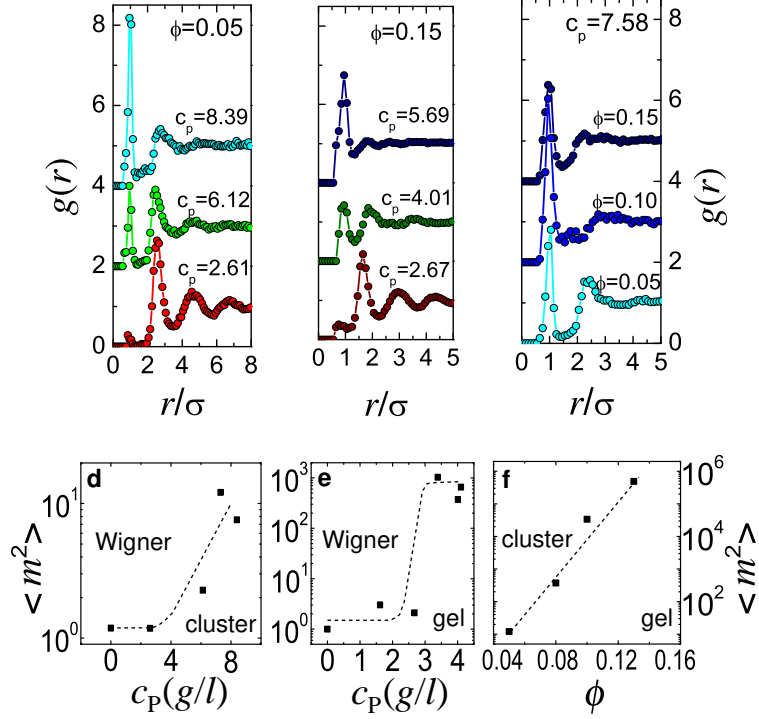


Figure 3: Dependences of $g(r)$ and $\langle m^2 \rangle$ on ϕ and c_p . (a) (path 1) shows the change in $g(r)$ across the Wigner-cluster glassy state transition. Vertical solid line indicates the peak at contact ($r = \sigma$), and dashed line indicates the first peak of $g(r)$ of the Wigner glassy state, corresponding to the average interparticle distance, and the second peak of $g(r)$ of the cluster glassy state, corresponding to the first shell of clusters. (b) (path 2) from a Wigner glassy to a gel state, and (c) (path 3) from a cluster glassy to a gel state. c_p is given in units of g/l. Data offset for clarity. (d) The change in $\langle m^2 \rangle$ along path 1 (at $\phi = 0.051$), (e) along path 2 (at $\phi = 0.151$), and along (f) path 3 (at $c_p = 7.58$ g/l). Dashed lines and shading are guides to the eye.

Let us now enquire as to the nature of the transitions between these glassy states. The transition between Wigner and cluster glassy states (path 1 in Fig. 1) is considered in more detail in Figs. 3(a) and (d), which show the radial distribution function $g(r)$ and the variance in the cluster size distribution $\langle m^2 \rangle$, where m is the number of particles per cluster. Rather than a sharp transition, the Wigner glassy state is unaffected by weak attractions; until the polymer concentration exceeds around $c_p = 4$ g/l there is no response in the size distribution. At higher c_p , there is an increase in (cluster) size, yet our data suggest that it occurs rather gradually, *i.e.*, passing from the Wigner to the cluster glassy state is a crossover rather

than a sharp transition: particles start to form small clusters above a certain threshold c_p and their size gradually increases with an increase in c_p . The gradual development of the peak at contact (at $r = \sigma$) in the $g(r)$ [Fig. 3(a)] further supports this observation. Note that the emergence of the peak at contact is a direct consequence of attractions. In equilibrium, the repulsive Wigner state (comprised of monomers) is expected to be a crystal. The same can apply to states of *monodisperse* clusters [28], however here the clusters are very polydisperse [see Fig. 1(a) and appendix], which leads to self-generated disorder, and intrinsically suppresses crystallization. This source of disorder is a consequence of a two-level organizational hierarchy, of colloids forming clusters and then clusters forming a glass which may be characteristic of a system of competing interactions with different lengthscales.

Proceeding to the transition between the Wigner glassy and gel states (path 2 in Fig. 1), we find a rather different scenario. Raising the colloid volume fraction to $\phi = 0.15$, the $g(r)$ [Fig. 3(b)] again shows the development of a peak at contact ($r = \sigma$) around $c_p = 4$ g/l. We recall that at lower ϕ , at a similar polymer concentration, clusters began to form [Fig. 3(a)]. For $\phi = 0.15$ this yields percolation [Fig. 1(j)], and a sharp transition to a gel state [Fig. 3(e)], accompanying a strong increase in $\langle m^2 \rangle$ by about three orders of magnitude. This is markedly different from the gradual continuous increase in $\langle m^2 \rangle$ for the Wigner-cluster glassy states [see Fig. 3(d)].

What happens in the case of the transition between cluster glassy and gel states? Path 3 in Fig. 1 is shown in Figs. 3(c) and (f). Unlike the previous transitions, here the polymer concentration is fixed at $c_p = 7.4$ g/l. In fact rather little change in the local structure is seen in the $g(r)$ analysis [Fig. 3(c)], and the variance in the cluster size increases continuously. Our results indicate that, in contrast to paths 1 and 2 in Fig. 1 the cluster glass-gel boundary is delineated by a percolation transition, rather than by local structural changes.

We also observed a novel aging mechanism in the cluster state. While aging is usually thought of in dynamic terms, here we present a structural mechanism for aging. This concerns the transition from a state of high potential energy, a tightly bound cluster of charged particles, to a smaller cluster, via cluster fission. We never observed any cluster fusion, and particle tracking shows a continuous rise in the population of small clusters as a function of time. The emission process occurs in less than 1/100 of the characteristic diffusion time, a much faster timescale than structural relaxation even in the absence of slow dynamics. This phenomenon is illustrated in Figs. 4(a) and (b). This cluster state

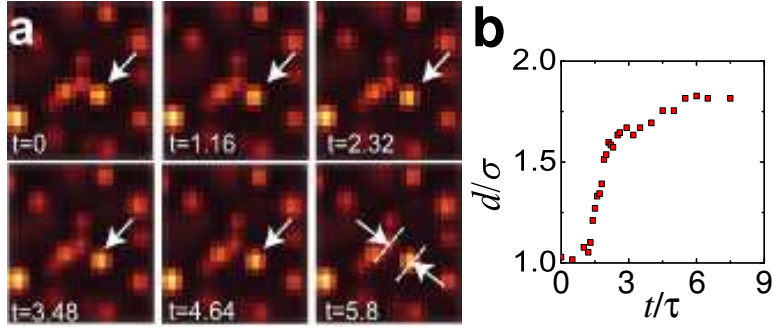


Figure 4: Aging mechanism of a cluster glassy state. (a) An emission process from an $m = 5$ to $m = 4$ cluster, as shown by arrows. Time t is expressed in units of $\tau/1000$ and the image width is $14\mu\text{m}$. (b) Separation of the emitted particle and cluster, as defined by arrows in (a), as a function of t .

suffers from a complex minimization problem involving the spatial distributions of colloids, counterions and polymers. The coupling between these three variables makes the potential energy landscape rather complex. This fission process allows us to directly observe a kinetic path from one local minimum to a neighboring minimum with a lower energy. Details of the cluster distribution and its time-evolution are available in the appendix.

Some comments on the colloidal interactions are in order. We have determined the colloid charge at low ϕ and $c_p = 0$. Using the parameters we calculate for the colloid charge, for this system we expect a potential at contact of several hundred $k_B T$, substantially in excess of the attractive forces mediated by the depletion attraction, $\sim 30 k_B T$ for $c_p = 4 \text{ gl}^{-1}$ at which we find clustering and gelation (see appendix). We believe that the charge is associated with the free surfaces of the colloids, and that clusters may have a markedly lower charge per colloid than do the isolated particles [29]. Calculations show that for such anisotropic charge distributions, the electrostatic repulsion is much reduced, enabling the clustering and gelation we observe [30].

IV. CONCLUSIONS

In closing, we found that the introduction of relatively strong, long-ranged repulsions to a colloidal dispersion with short-range attractions, generates novel glassy states, such as the cluster glassy state, and drastically transforms behavior, at that most fundamental

of levels: the ability of the system to relax locally. For a system of short-ranged attractive interactions, without strong, long-ranged repulsions, it is possible to distinguish the repulsive hard-sphere glass and the attractive glass, as depicted in Fig. 1(g) [11], but there the change in the structure is rather subtle [27]. In contrast, the transitions between cluster glassy and gel states and between Wigner glassy and gel states both accompany significant structural changes from single particle to compact clusters and a percolating network, respectively. The observed behavior can be interpreted as the interplay of a Wigner glassy state dominated by the long-range repulsions with formation of clusters driven by short-range attractions [17] and their percolation for gelation. Like the neutral system, there appear to be two drivers of arrest: the gel is driven by attractions and both Wigner and cluster glassy states are driven by repulsion. The effect of long-ranged repulsions on the state diagram of a system with short-ranged attractions is an interesting fundamental problem; at intermediate repulsions a cluster fluid emerges [20–22]. Since protein solutions are also understood to exhibit comparable interactions, we conclude that it is at least reasonable to suppose that equilibrium cluster phases may be found [16, 31], and perhaps even cluster glasses.

The authors are grateful to Didi Derks, Rob Jack and Matthias Schmidt for a critical reading of the manuscript. CLK thanks the Deutscher Akademischer Austauschdienst for financial assistance. CPR acknowledges the Royal Society for financial support. HT acknowledges a Grant-in-Aid from the Ministry of Education, Culture, Sports, Science and Technology, Japan.

Appendix

Samples and experimental methods. We used poly(methyl methacrylate) (PMMA) colloids sterically stabilized with polyhydroxyl steric acid. The colloids were labelled with the fluorescent dye rhodamine isothiocyanate and had a diameter $\sigma = 1.95 \mu\text{m}$ with around 5% polydispersity. Solvents and polymers were used as received. The polymer used was polystyrene, with a molecular weight of $M_w = 2.06 \times 10^7$. To closely match the colloid density and refractive index we used a solvent mixture of cis-decalin and cyclohexyl bromide. Due to the refractive index matching, the van der Waals interactions are reduced to a fraction of the thermal energy $k_B T$ (k_B : Boltzmann’s constant; T : temperature) and neglected. We confined the samples to thin (100 μm) capillaries which provided access to the entire sample,

but confirmed, with experiments using larger 500 μm cells, that this confinement has little effect upon the behavior. Prior to each experiment, sample vials were washed with copious quantities of ethanol, and carefully dried. Dry colloids were then added, and dispersed in solvent, with the polymer solution added last. The data was collected on a Leica SP5 confocal microscope, fitted with a resonant scanner. We determined the co-ordinates of each particle with a precision of around 100 nm [23]. Connectivity was determined by setting the bond length equal to the sum of the range of the attractive interactions and the tracking error. Our conclusions are insensitive to the exact value of the bond length. The time for a colloid to diffuse one radius is given by the Stokes-Einstein relation as $\tau = 3\pi\eta\sigma^3/(4k_{\text{B}}T)$ where η is the viscosity. This we measure independently as a function of polymer concentration using a Rheologica Instruments Stress Tech rheometer.

Determining the interactions between the colloids. The behavior we have observed is driven by competing attractive and repulsive interactions. We shall begin our discussion of the potentials by considering the attractive depletion interaction. We have used a polymer of $M_w = 2.06 \times 10^7$. Here we used a ‘good’ solvent, and in detailed studies using the same solvent-polymer mixture, we found good agreement with the Asakura-Oosawa (AO) theory [32], assuming polymer swelling such that the radius of gyration R_G is increased by 35%. We therefore assumed a similar degree of swelling here, such that $R_G \approx 190$ nm, leading to a polymer-colloid size ratio $q = 2R_G/\sigma \approx 0.19$, which sets the range of the attractive interaction. For the dilute polymer regime, little deviation is expected from AO theory [32], even in the case of some polymer swelling (non-ideality) [33]. Furthermore, although we add sufficient polymer that some of our samples are just into the semi-dilute regime, relatively little deviation is expected from AO theory for these parameters [33]. At the level of this work, therefore, we treat the attractions with AO theory which leads to a pair interaction between two hard colloidal spheres in a solution of ideal polymers which reads

$$\beta u_{\text{AO}}(r) = \begin{cases} \infty & \text{for } r < \sigma \\ \frac{\pi(2R_G)^3 z_{\text{PR}} (1+q)^3}{6 q^3} & \text{for } r \geq \sigma < \sigma + (2R_G) \\ \times \left\{ 1 - \frac{3r}{2(1+q)\sigma} + \frac{r^3}{2(1+q)^3\sigma^3} \right\} & \text{for } r \geq \sigma + (2R_G) \\ 0 & \text{for } r \geq \sigma + (2R_G) \end{cases} \quad (1)$$

where β is $1/k_{\text{B}}T$. The polymer fugacity z_{PR} is equal to the number density ρ_{PR} of ideal

polymers in a reservoir at the same chemical potential as the colloid-polymer mixture. This corresponds to a contact potential of $7.0 k_B T$ per g/l of polymer reservoir concentration.

Determining the electrostatic interactions in non-aqueous colloidal dispersions is a non-trivial task [23, 34], as the charge and ionic strength are very small, although they still lead to significant interactions. The interactions have nevertheless been found to be well described by the screened Coulomb or Yukawa interaction, which reads

$$\beta u_{YUK}(r) = \begin{cases} \infty & \text{for } r < \sigma \\ \beta \epsilon \frac{\exp(-\kappa(r-\sigma))}{r/\sigma} & \text{for } r \geq \sigma \end{cases} \quad (2)$$

where r is the center to center separation of the two colloids. The contact potential is given by

$$\beta \epsilon = \frac{Z^2}{(1 + \kappa\sigma/2)^2} \frac{l_B}{\sigma}, \quad (3)$$

where Z is the colloid charge, κ is the inverse Debye screening length and l_B is the Bjerrum length.

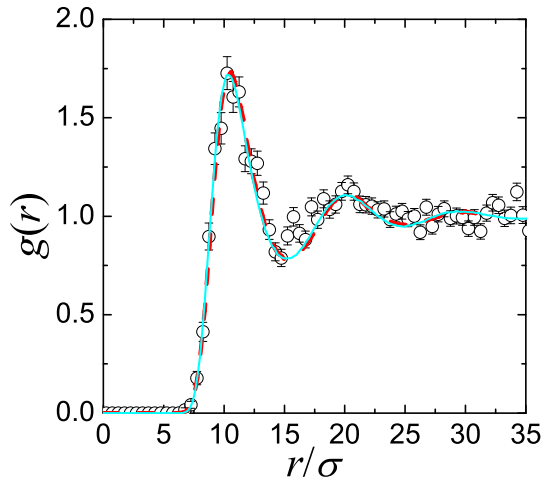
One may thus assume interactions between the colloids take the form of a short-range ‘depletion’ attraction and long-ranged screened Coulomb repulsion, and a nearly hard core. Both have been measured in nearly identical systems and found to be in good agreement with theory [23, 24]. Here we have determined the colloid charge and ionic strength by comparison of the measured $g(r)$ with one obtained from Monte Carlo simulation according to a Yukawa potential [24] in the ergodic fluid part of the state diagram ($\phi = 4.8 \times 10^{-4} \pm 2 \times 10^{-5}$, $c_p = 0$) to be $Z \approx 600 \pm 200 e$ where e is the elementary unit of charge, and the inverse Debye length $\kappa\sigma \approx 1 \pm 0.4$. The radial distribution function $g(r)$ fitting is shown in SFig. 1. This method is found to be consistent with electrophoretic measurements [24]. The values we obtain for the colloid charge are somewhat (up to 25%) higher than those quoted previously in literature where samples were prepared using dry colloids [24, 34]. For these parameters mode-coupling theory predicts vitrification at higher volume fractions [25]. However, this analysis poses a significant question: the contact potential between two such colloids is $\beta \epsilon \sim 1000$. This is much greater than the strength of the attraction induced by the polymer. Throughout the measurements we find that clustering of gelation occurs at a polymer concentration around $c_p = 4.0 \text{ gl}^{-1}$, which corresponds to a contact potential of around $30 k_B T$ [Eq. (1)].

We are reasonably confident about our understanding of the attraction induced by the polymer [23]. We speculate that the charge is in fact different between the isolated colloids

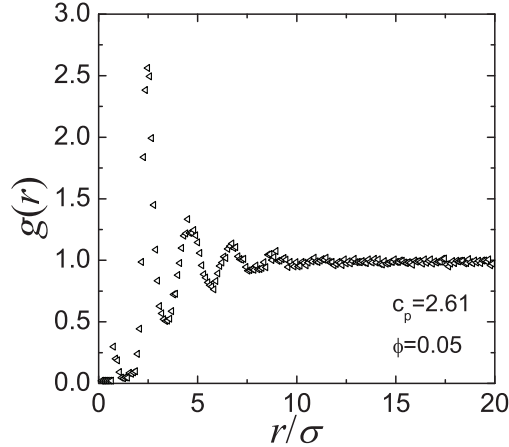
upon which measurements of the charge Z are based and colloids found in clusters, consistent with behavior we observed in a similar cluster-forming system [29] and values quoted in the literature [16, 20, 21]. Alternatively, non-pairwise additivity with these long-ranged repulsions leading to a reduction in apparent repulsion may play an important role [35]. In all of these cases, the quoted values for the repulsive interactions are stronger than the depletion induced attractions.

Pointers to an understanding of the underlying cause for this discrepancy may be found in measurements that indicate a reduction in charge per colloid upon clustering [29]. Moreover, if this charge were inhomogeneously distributed, a further reduction in repulsions is to be expected [30] upon which clustering due to polymer-induced attractions is not unreasonable. Further work is in progress to elucidate the charging mechanism, and possible charge anisotropy, however, we note that the weak levels of electrostatic charging in these apolar systems severely hamper a full understanding.

However, the strength of the depletion interaction, as gauged by its strength at contact [Eq. (1)] is rather stronger here than in systems where the charge is screened [10, 36]. Comparing the minimum polymer concentration required to form a gel, we find around a contact potential of $\beta u_{AO} \approx 11$. When the electrostatic repulsions are screened one finds $\beta u_{AO} \approx 3$ for attractions of comparable range ($q=0.18$) [36], rising slightly to $\beta u_{AO} \approx 5$ for shorter-ranged attractions [10]. Previous work on charged systems with a much short-ranged attraction ($q = 0.04$) suggests a threefold increase in the contact potential βu_{AO} required for gelation [21] relative to systems where the charge is screened.



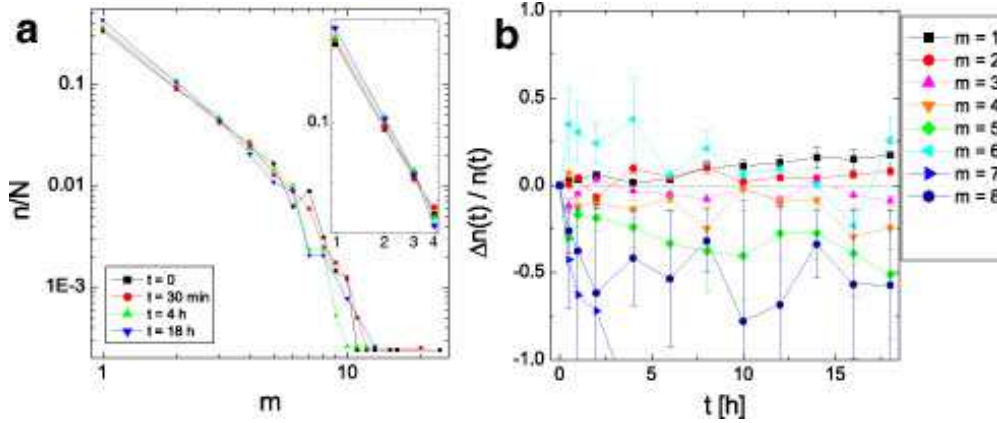
SFig. 1: Analysis of $g(\mathbf{r})$. Radial distribution function. Dashed red line corresponds to a colloid charge $Z = 400$, solid cyan to $Z = 800$. We assumed that the Debye screening length was dominated by the colloidal counterions, in other words the system is close to the salt-free limit. This leads to a fitting which depends solely upon Z . Lower values of Z gave poor fits, higher values of Z led to crystallization.



SFig. 2: $g(\mathbf{r})$ for repulsive glass. Decay of the spatial density correlation at long range suggests an absence of crystallization and that the state is a repulsive Wigner glass. Polymer concentration c_p is given in units of g/l.

On crystallization. Occasionally we found that, rather than a Wigner glassy state [Fig. 1(e)], the system in fact crystallized [Fig. 1(f)]. That similar samples may either crystallize or vitrify suggests multiple paths through the free-energy landscape, as found in some clay suspensions [37]. Alternatively, the systems size we study allow the possibility of a variation in nucleation time between different experiments, leading to the observation of crystallization in a limited set of samples.

The fact that the crystal forms at all also suggests that the increase in ϕ may promote ordering and reduce the glass-forming ability of the system. We never observed an ordered phase for $\phi < 0.2$, this is further supported by the radial distribution function in SFig. 2 which shows an absence of long-ranged order for the repulsive glass. That we only found a Wigner glass at low ϕ , an apparently shallower quench, but occasionally a crystal at higher ϕ , is interesting, and may be explained by a stronger screening of the electrostatic repulsion due to a higher concentration of counter ions at higher ϕ , leading to ‘harder’ interactions which promote crystallization.



SFig. 3: Cluster distribution and aging mechanism. **a**, shows the variation in cluster size distribution over time. The inset shows the distribution for clusters of size $m < 5$. n denotes the number of clusters, N the number of coordinates (particles) found. m gives the size of clusters. **b**, shows the evolution of different cluster sizes, where $\Delta n(t) = n(t) - n(0)$. Note the increase in the population of $m = 6$ at early times.

On the absence of mesoscopic ordered structures. Here we note that a considerable literature exists, predicting pattern-formation and lamellae-like phases in systems with competing interactions [6, 17]. We see little periodicity in the system studied here. In the case of the cluster glass, this is likely due to extremely slow equilibration to a monodisperse cluster phase which could then potentially form a cluster crystal [28]. Our experiments run for up to two weeks, and there was no indication of crystalline ordering, moreover the cluster distribution was still very polydisperse on this timescale. The behavior up to 18 hours is shown in SFig. 3.

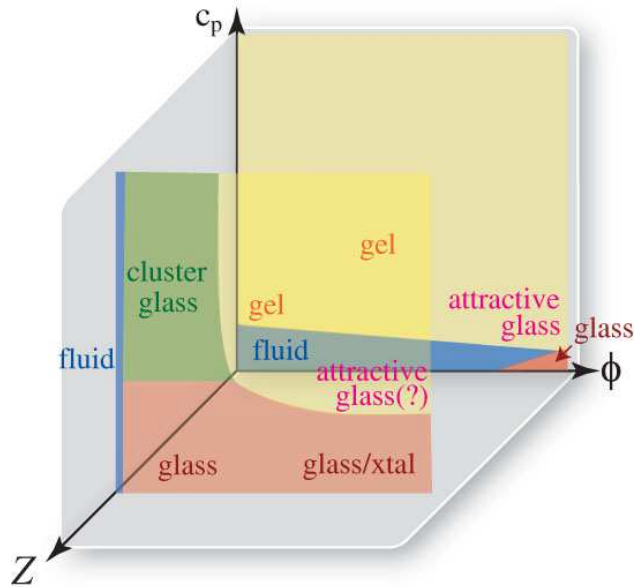
In the gel, on the other hand, we believe that the bicontinuous network is slow to break and re-arrange due to the connectivity [38], as would be required to form a lamellar type structure. Another important difference in comparing the gel state with for example, microemulsions, lies in the arrested nature of the ‘colloid’-rich phase. Microemulsions are thus able to reorganize locally in a way that a system with short-ranged attractions, is not.

Dependence of the state diagram of multiple dynamic arrested states upon the strength of electrostatic interactions. The state diagram of multiple dynamic arrested states for varying strengths of the electrostatic interactions is shown in SFig. 4. Upon reducing the strength of the electrostatic interaction, one expects to recover the behavior

of hard spheres with a short-ranged attractive interaction [11]. That is to say, fluid, gel, attractive and hard sphere glasses. Here we discuss the differences this phase diagram relevant to neutral colloids to the strongly charged case presented here. Note that we consider the case of no added salt such that the electrostatics are unscreened.

The effect of increasing electrostatic repulsions is as follows. When the colloid charge Z is small, a fluid (blue), gel, attractive glass (yellow) and repulsive glass (red) states are found [11]. Our study suggests that increasing the electrostatic repulsions leads to the system studied here, with a significant extension of the repulsive glass to low densities, such that we find a direct repulsive glass-gel transition. This is quite different from the fluid-gel transition in the case of small Z . Moreover the enhancement of repulsions due to the electrostatics leads to an increase in the amount of polymer required for gelation.

We furthermore see the emergence of a cluster glassy state (green), which is not found for neutral systems. Nonergodicity stems from connectivity in the case of the gel and caging for single particles and clusters, respectively, for the repulsive and cluster glasses. For a high colloid volume fraction, there may also be an attractive glass state, although such a high volume fraction region was not investigated in this study. We emphasize that for large Z an ergodic state exists only for a very low colloid volume fraction and most state points form non-ergodic disordered states. It is an intriguing, fundamental question how the state diagram evolves between these two extremes.



SFig. 4: 3D state diagram. The state diagrams for two extremes, negligible and strong

electrostatic interactions ($Z = 0$ and large Z) are indicated. The former has been established in [11], while the latter is a schematic of Fig. 1. See the text for details.

- [1] M. Seul and D. Andelman. Domain shapes and patterns - the phenomenology of modulated phases. *Science*, 267:476–483, 1995.
- [2] E. Dagotto. Complexity in strongly correlated electronic systems. *Science*, 309:257–262, 2005.
- [3] Perez-Garcia Horowitz and Piekarewicz. Neutrino-”pasta” scattering: The opacity of nonuniform neutron-rich matter. *Phys. Rev. C*, 69:045804, 2004.
- [4] V.J. Emery and S.A. Kivelson. Frustrated electronic phase separation and high-temperature superconductors. *Physica C*, 209:597–621, 1993.
- [5] F. Sciortino and P. Tartaglia. Glassy colloidal systems. *Advances in Physics*, 54(6):471–524, 2005.
- [6] M. Tarzia and A. Coniglio. Pattern formation and glassy phase in the phi4 theory with a screened electrostatic repulsion. *Phys. Rev. Lett.*, 96:075702, 2006.
- [7] F. Sciortino, S. Mossa, E. Zaccarelli, and P. Tartaglia. Equilibrium cluster phases and low-density arrested disordered states: The role of short- range attraction and long-range repulsion. *Phys. Rev. Lett.*, 93:055701, 2004.
- [8] G. Tarjus, S .A. Kivelson, Z. Nussinov, and P. Viot. The frustration-based approach of supercooled liquids and the glass transition: a review and critical assessment. *J. Phys.: Condens. Matter*, 17:R1143–R1182, 2005.
- [9] H. Tanaka, J. Meunier, and D. Bonn. Nonergodic states of charged colloidal suspensions: Repulsive and attractive glasses and gels. *Phys. Rev. E.*, 69:031404, 2004.
- [10] P. J. Lu, E. Zaccarelli, F. Ciulla, A. B. Schofield, F. Sciortino, and D. A. Weitz. Gelation of particles with short-range attraction. *Nature*, 453:4990–503, 2008.
- [11] K. N. Pham, A. M. Puertas, J. Bergenholtz, S. U. Egelhaaf, A. Moussaid, P. N. Pusey, A. Schofield, M. E. Cates, M. Fuchs, and Poon W. C. K. Multiple glassy states in a simple model system. *Science*, 296:104–106, 2002.
- [12] Y. Gao and M.L. Kilfoil. Direct imaging of dynamical heterogeneities near the colloid-gel transition. *Phys. Rev. Lett.*, 99:078301, 2007.
- [13] E. B. Sirota, H. D. Ou-Yang, S. K. Sinha, P. M. Chaikin, J. D. Axe, and Y. Fujii. Complete

- phase diagram of a charged colloidal system. *Phys. Rev. Lett.*, 62:1524–1527, 1989.
- [14] E. Zaccarelli. Colloidal gels: Equilibrium and non-equilibrium routes. *J. Phys.: Condens. Matter*, 19:323101, 2007.
- [15] C. Semmrich, T. Storz, J. Glaser, R. Merkel, A. R. Bausch, and K. Kroy. Glass transition and rheological redundancy in f-actin solutions. *Proc. Nat. Acad. Sci.*, 104:20199–20203, 2008.
- [16] A. Stradner, H. Sedgwick, F. Cardinaux, W.-C.K. Poon, S.U. Egelhaaf, and P. Schurtenberger. Equilibrium cluster formation in concentrated protein solutions and colloids. *Nature*, 432:492–495, 2004.
- [17] J. Groenewold and W.K. Kegel. Anomalously large equilibrium clusters of colloids. *J. Phys. Chem. B.*, 105:11702–11709, 2001.
- [18] K. Kroy, W.C.K. Poon, and M.E. Cates. Cluster mode-coupling approach to weak gelation in attractive colloids. *Phys. Rev. Lett.*, 92:148302, 2004.
- [19] J. C. Fernandez Toledano, F. Sciortino, and E. Zaccarelli. Colloidal systems with competing interactions: from an arrested repulsive cluster phase to a gel. *Soft Matter*, 2009.
- [20] A. I. Campbell, V. J. Anderson, J. S. van Duijneveldt, and P. Bartlett. Dynamical arrest in attractive colloids: The effect of long-range repulsion. *Phys. Rev. Lett.*, 94(20):208301, May 2005.
- [21] C. J. Dibble, M. Kogan, and M. J. Solomon. Structure and dynamics of colloidal depletion gels: Coincidence of transitions and heterogeneity. *Phys. Rev. E.*, 74:041403, 2006.
- [22] H. Sedgwick, S.U. Egelhaaf, and W.-C.K. Poon. Clusters and gels in systems of sticky particles. *J. Phys.: Condens. Matter*, 16:S4913–S4922, 2004.
- [23] C. Patrick Royall, Ard A. Louis, and Hajime Tanaka. Measuring colloidal interactions with confocal microscopy. *The Journal of Chemical Physics*, 127(4):044507, 2007.
- [24] C.P. Royall, M.E. Leunissen, A-P. Hynninen, M. Dijkstra, and A. van Blaaderen. Re-entrant melting and freezing in a model system of charged colloids. *J. Chem. Phys.*, 124:244706, 2006.
- [25] S.K. Lai, W.J. Ma, W. van Meegen, and I.K. Snook. Liquid-glass transition phase diagram for concentrated charge-stabilized colloids. *Phys. Rev. E.*, 56:766–769, 1997.
- [26] E. Zaccarelli, S. Andreev, F. Sciortino, and D. R. Reichman. Numerical investigation of glassy dynamics in low-density systems. *Phys. Rev. Lett.*, 100:195701, 2008.
- [27] N.B. Simeonova, R.P.A. Dullens, D.G.A.L. Aarts, H.N.W. de Villeneuve, V.W.A. Lekkerkerker, and W.K. Kegel. Devitrification of colloidal glasses in real space. *Phys. Rev. E.*,

- 73:041401, 2006.
- [28] B. M. Mladek, D. Gottwald, G. Kahl, M. Neumann, and C. N. Likos. Formation of polymorphic cluster phases for a class of models of purely repulsive soft spheres. *Phys. Rev. Lett.*, 96:045701, 2006.
 - [29] C. L. Klix, K. Murata, H. Tanaka, S. Williams, A. Malins, and C. P. Royall. The role of weak charging in metastable colloidal clusters. *ArXiv cond-mat.soft*, page 0905.3393, 2009.
 - [30] N. Hoffman, C. N. Likos, and J. P. Hansen. Linear screening of the electrostatic potential around spherical particles with non-spherical charge patterns. *Molecular Physics*, 102:857–867, 2004.
 - [31] A. Shukla, E. Mylonas, E. Di Cola, S. Finet, P. Timmins, T. Narayanan, and D. I. Svergun. Absence of equilibrium cluster phase in concentrated lysozyme solutions. *Proc. Nat. Acad. Sci.*, 105:5075–5080, 2008.
 - [32] S. Asakura and F. Oosawa. On interaction between 2 bodies immersed in a solution of macromolecules. *J Chem Phys*, 22(7):1255–1256, 1954.
 - [33] A. A. Louis, P. G. Bolhuis, E. J. Meijer, and J. P. Hansen. Polymer induced depletion potentials in polymer-colloid mixtures. *J. Chem. Phys.*, 117:1893–1907, 2002.
 - [34] C. P. Royall, M. E. Leunissen, and A. van Blaaderen. A new colloidal model system to study long-range interactions quantitatively in real space. *Journal of Physics, Condensed Matter*, 15(48):S3581–S3596, December 2003.
 - [35] J. W. Merrill, S. K. Sainis, and E. R. Dufresne. Many-body electrostatic forces between colloidal particles at vanishing ionic strength. *ArXiv:cond-mat.soft*, page 0907.0721, 2009.
 - [36] C. P. Royall, S. R. Williams, T. Ohtsuka, and H. Tanaka. Direct observation of a local structural mechanism for dynamic arrest. *Nature Mater.*, 7:556–561, 2008.
 - [37] S. Jabbari-Farouji, G.H. Wegdam, and D. Bonn. Gels and glasses in a single system: Evidence for an intricate free-energy landscape of glassy materials. *Phys. Rev. Lett.*, 99:065701, 2007.
 - [38] H. Tanaka and T. Araki. Spontaneous coarsening of a colloidal network driven by self-generated mechanical stress. *Europhys. Lett.*, 79:58003, 2007.